PROCEEDINGS OF SCIENCE

Light curve analysis of classical novae: free-free emission vs photospheric emission

Izumi Hachisu*
Department of Earth Science and Astronomy, College of Arts and Sciences, The University of Tokyo, Tokyo 153-8902, Japan
E-mail: hachisu@ea.c.u-tokyo.ac.jp

Mariko Kato
Department of Astronomy, Keio University, Yokohama 211-8521, Japan

We analyzed light curves of relatively slower novae, based on an optically thick wind theory of nova outbursts. In slower novae, we must take into account photospheric emission as well as free-free emission because their wind mass loss rates are smaller and the brightness of free-free emission is as faint as photospheric emission. We calculated model light curves of free-free plus photospheric emission for various WD masses and various chemical compositions of the envelopes, and fitted them reasonably with observational data of optical, near-infrared (NIR), and UV bands. From light curve fittings, we estimated their absolute magnitudes, distances, and WD masses. In the fast novae V1668 Cyg and V1974 Cyg, free-free emission dominates the spectrum in the optical and NIR regions, so the optical and NIR light curves follow the universal decline law. In slower novae PW Vul and V705 Cas, free-free emission still dominates the spectrum in the optical and NIR bands but photospheric emission contributes significantly to the spectrum in the later phase. In very slow novae such as RR Pic and V723 Cas, photospheric emission dominates the spectrum rather than free-free emission. These photospheric emission effect makes a deviation from the universal decline law and therefore a systematic deviation from the proposed maximum magnitude vs rate of decline (MMRD) relation.

The Golden Age of Cataclysmic Variables and Related Objects - III, Golden2015
7-12 September 2015
Palermo, Italy

*Speaker.

PoS(Golden2015)053

1. Introduction

Based on their optically thick wind model, Hachisu & Kato [1] found that, in terms of free-free emission, optical and near-infrared (NIR) light curves of several novae follow a universal decline law. Their time-normalized light curves are almost independent of the WD mass, chemical composition of ejecta, and wavelength. Hachisu & Kato [1] also found that their UV 1455 Å model light curves [2], interpreted as photospheric blackbody emission, are also time-normalized by the same factor as in the optical and NIR light curves. Using the fact that the time-scaling factor is closely related to the WD mass, Hachisu & Kato and their collaborators determined the WD mass and other parameters for a number of well-observed novae [3, 4, 5, 6, 7].

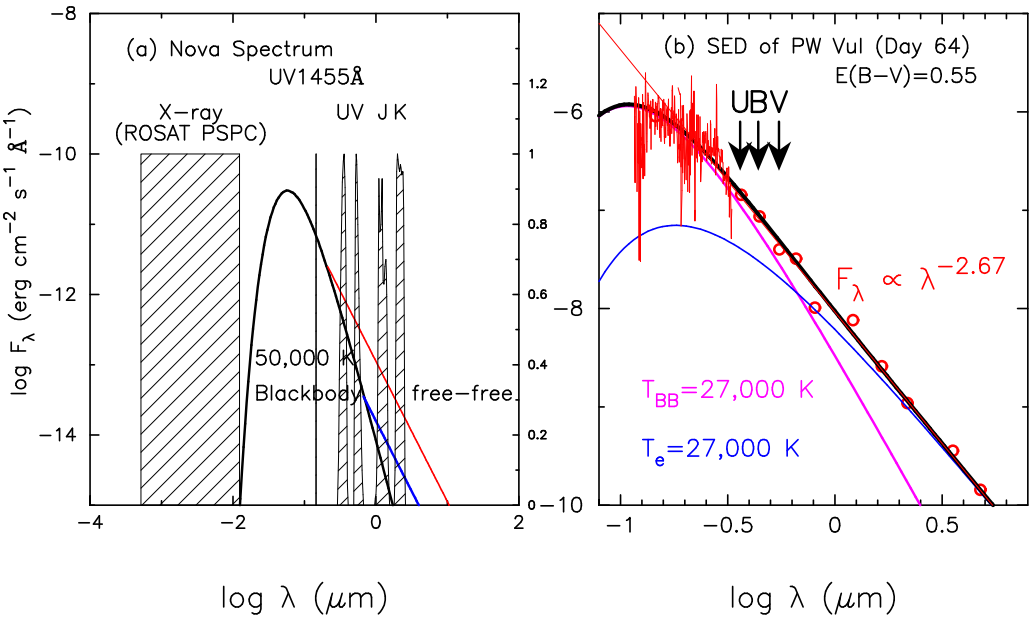

Figure 1: (a) An illustration of spectral energy distribution (SED) of a classical nova with a photospheric temperature of $T_{\rm ph} = 50{,}000$ K as well as various passbands of the photometric filters. The UV 1455Å (1445–1465Å) and supersoft X-ray (0.1–2.4 keV) fluxes are calculated from blackbody spectrum in our model while the U, (B), V, J, (H), and K magnitudes are calculated from the sum of free-free and blackbody emissions. If the mass-loss rate is large, the flux of free-free emission dominates the spectrum in the optical and IR region as indicated by a red solid line. If it is small, the flux of free-free emission may dominate only in the IR region as indicated by a blue line. (b) SED of PW Vul 64 days after outburst.

Figure 1(a) shows a schematic illustration of nova continuum spectrum superposed on the various wavelength bands. The black thick solid line shows a 5000 K blackbody (BB) spectrum. Free-free emission is shown by two (red and blue thick solid lines). One is for a high wind mass loss rate (red solid) and the other for a low wind mass loss rate (blue solid). In general, slower novae are related to less massive WDs which blow optically thick winds with relatively smaller wind mass loss rates [8]. The total flux is the summation of of the free-free and blackbody emission. Thus, in novae with strong winds, free-free emission dominates but in novae with weak winds, blackbody emission contributes significantly to the spectrum in the optical and NIR regions. The universal decline law is theoretically derived by Hachisu & Kato [1] based on the free-free emission. This

means that the universal decline law can be applied to novae with strong winds, but for novae with weak winds it can be done only for light curves of NIR region or longer wavelength.

Figure 1(b) shows the decomposition of the PW Vul spectrum 64 days after the outburst into two components, $F_\lambda = B_\lambda + S_\lambda$, of the blackbody ($B_\lambda$, magenta solid line) and optically thick free-free emission (S_λ, blue solid line). See Equations (2) and (3) of Hachisu & Kato [9]. Here, we show the decomposited spectrum assuming an extinction of $E(B-V) = 0.55$ for PW Vul. When the wind mass loss rate is small, the contribution of free-free emission is relatively small. We may conclude that, in V band, the free-free flux is comparable to the blackbody emission from the pseudophotosphere. We see that the blackbody emission gives a good approximation to the UV region and the free-free emission is a good fit to the IR region. In the region between them, the contributions from the blackbody and free-free components are comparable.

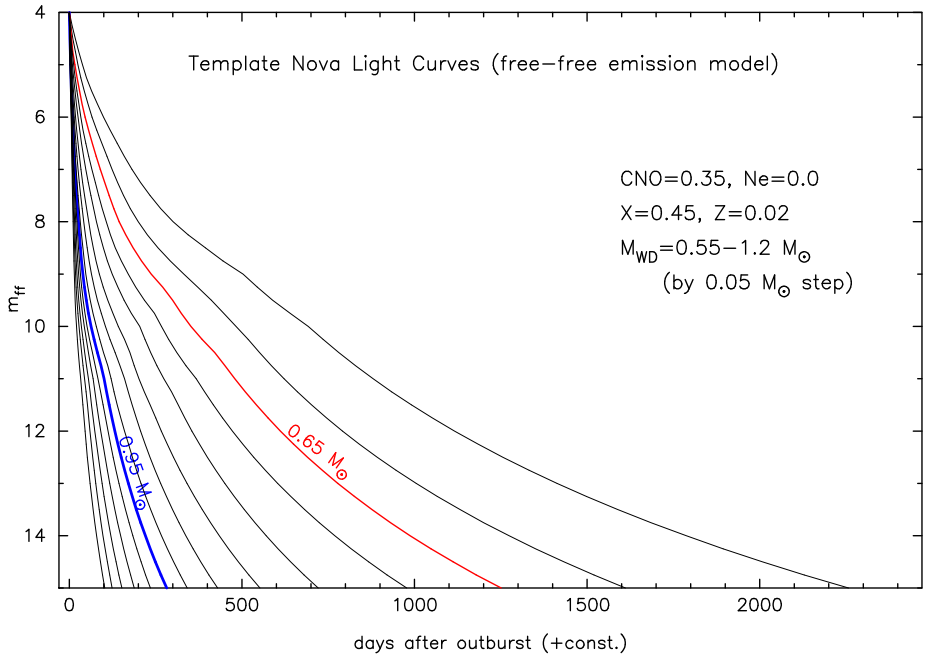

Figure 2: Free-free emission model light curves for the chemical composition of CO nova 3 (taken from Hachisu & Kato [10]).

2. Theoretical light curve model of novae

We calculate the flux of free-free emission from

$$F_\nu \propto \int N_{\rm e} N_{\rm i} dV \propto \int_{R_{\rm ph}}^{\infty} \frac{\dot{M}_{\rm wind}^2}{v_{\rm wind}^2 r^4} r^2 dr = \frac{\dot{M}_{\rm wind}^2}{v_{\rm ph}^2 R_{\rm ph}} \tag{2.1}$$

for optically thin ejecta outside the pseudophotosphere, where F_ν is the flux at the frequency ν. For Kato & Hachisu's [8] optically thick nova wind models, we have $N_e \propto \rho_{\rm wind}$ and $N_i \propto \rho_{\rm wind}$, where $\rho_{\rm wind}$ is the density of winds, $\dot{M}_{\rm wind}$ is the wind mass-loss rate, $v_{\rm ph}$ and $R_{\rm ph}$ are the velocity and radius at the pseudophotosphere. Here, we integrate Equation (2.1) outside the photosphere assuming that the wind velocity is $v_{\rm wind} = v_{\rm ph}$ (=constant in space) outside the photosphere and

using the relation of continuity, $\rho_{\rm wind} = \dot{M}_{\rm wind}/4\pi r^2 v_{\rm wind}$. Note that the flux F_ν is independent of the frequency ν in the case of optically thin free-free emission. In Figure 2, we plot such an example of model light curves of free-free emission for the chemical composition of "CO nova 3" ($X = 0.45$, $Y = 0.16$, $X_{\rm CNO} = 0.35$, $X_{\rm Ne} = 0.0$, $Z = 0.02$; see Table 2 of Hachisu & Kato [10] for the adopted sets of chemical composition). The details of calculations are presented in Hachisu & Kato [1, 4, 9, 10]. The magnitudes of our free-free emission model light curves are tabulated in Table 4 of Hachisu & Kato [10].

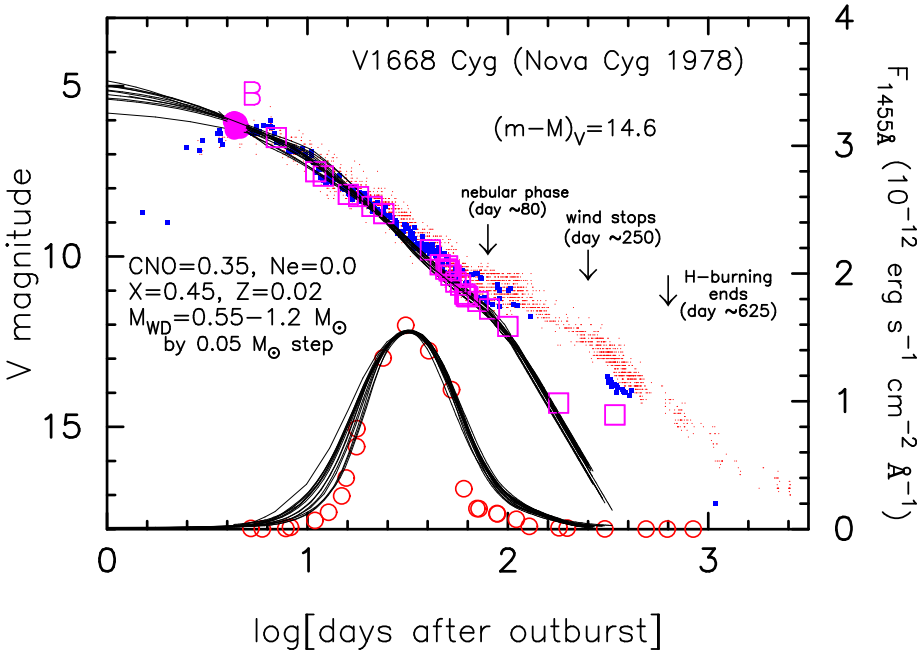

Figure 3: Universal shape of free-free emission model light curves for the chemical composition of CO nova 3 (taken from Hachisu & Kato [10]).

The free-free emission model light curves in Figure 2 have strong similarity in their shapes, so we overlap them by properly squeezing/stretching along time. We show such an example of light curves in Figures 3 for the light curves in Figure 2. Hachisu & Kato [1] called this similarity "the universal decline law."

Using the properties of free-free emission and the universal decline law, Hachisu & Kato [4, 9, 10] obtained the absolute magnitudes of these free-free emission model light curves as

$$\begin{aligned} M_V^{\{M_{\rm WD}\}}(t) &= m_V^{\{M_{\rm WD}\}}(t) - (m-M)_{V,\rm V1668\ Cyg} \\ &= 2.5\log f_{\rm s} - 2.5\ \log \left[\frac{\dot{M}_{\rm wind}^2}{v_{\rm ph}^2 R_{\rm ph}}\right]_{(t/f_s)}^{\{0.98\ M_\odot\}} \\ &\quad + K_V - (m-M)_{V,\rm V1668\ Cyg} \\ &= m'^{\{M_{\rm WD}\}}_V(t/f_s) + 2.5\log f_{\rm s} - (m-M)_{V,\rm V1668\ Cyg}, \end{aligned} \tag{2.2}$$

from the distance modulus of V1668 Cyg, i.e., $(m-M)_{V,\rm V1668\ Cyg} = 14.6$. Here, $m'^{\{M_{\rm WD}\}}_V(t')$ is the

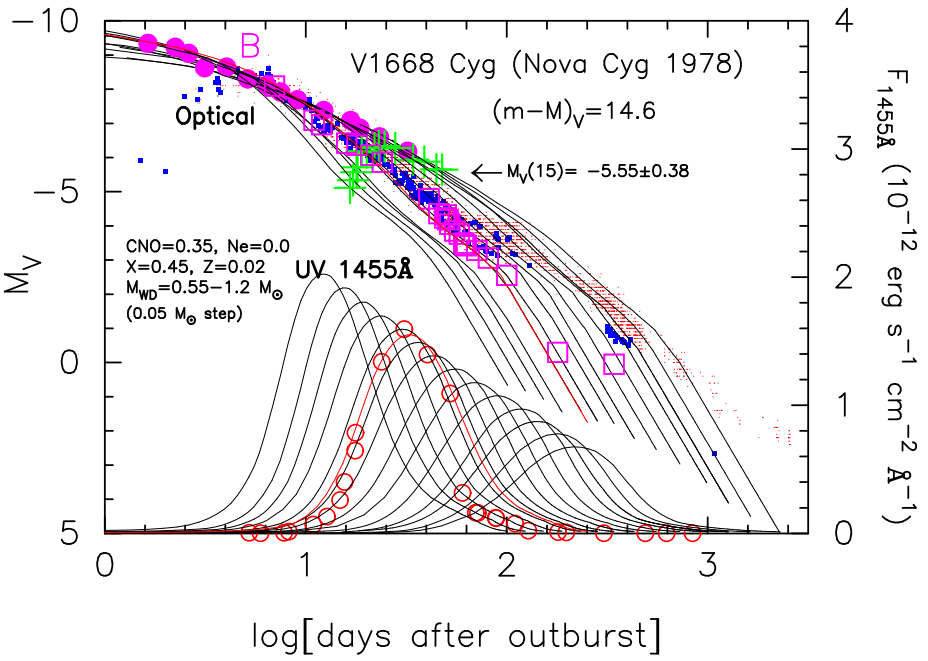

Figure 4: Absolute magnitude of free-free emission model light curves for the chemical composition of CO nova 3 (taken from Hachisu & Kato [10]).

universal decline shape in Figure 3, and t_s is the stretching factor of a nova light curve. Then, we obtain the absolute magnitudes of each free-free emission model light curve as shown in Figure 4.

3. Results

Figure 5 show the optical and UV light curves of V1668 Cyg and our model light curves. See Hachisu & Kato [10] for each source of the data. Our model light curves of V and UV 1455Å bands nicely fit with the observation. The photospheric (blackbody) emission contributes very little (at most ~ 0.2 mag) to the total flux.

It should be noted that our model light curve reasonably fits with the early V light curve but deviates from the visual and V observation in the nebular phase. On the other hand, our free-free model light curve fits well with the intermediate y-band magnitudes even in the later phase. This deviation in visual magnitudes is owing to strong emission lines such as [OIII], which are not included in our model. The intermediate y-band filter avoids strong emission lines such as [OIII] in the nebular phase.

Figure 6 also show the optical, UV, and soft X-ray light curves of V1974 Cyg and our model light curves. See also Hachisu & Kato [10] for each source of the data. Our model light curves of V, UV 1455Å, and supersoft X-ray bands nicely fit with the observation.

We obtain two distance-reddening relations toward V1668 Cyg from the two model light curve fittings in Figure 5 and plot them in Figure 7(a), where the V-fit is the blue lines and the UV 1455 Å-fit is the magenta lines. We further plot other distance-reddening relations toward V1668 Cyg; that given by Slavak et al. [12] (large red filled circles), that given by Marshall et al. [13], and that given by Green et al. [14]. All these trends/lines cross at $d \sim 5.4$ kpc and $E(B-V) \sim 0.30$. Therefore,

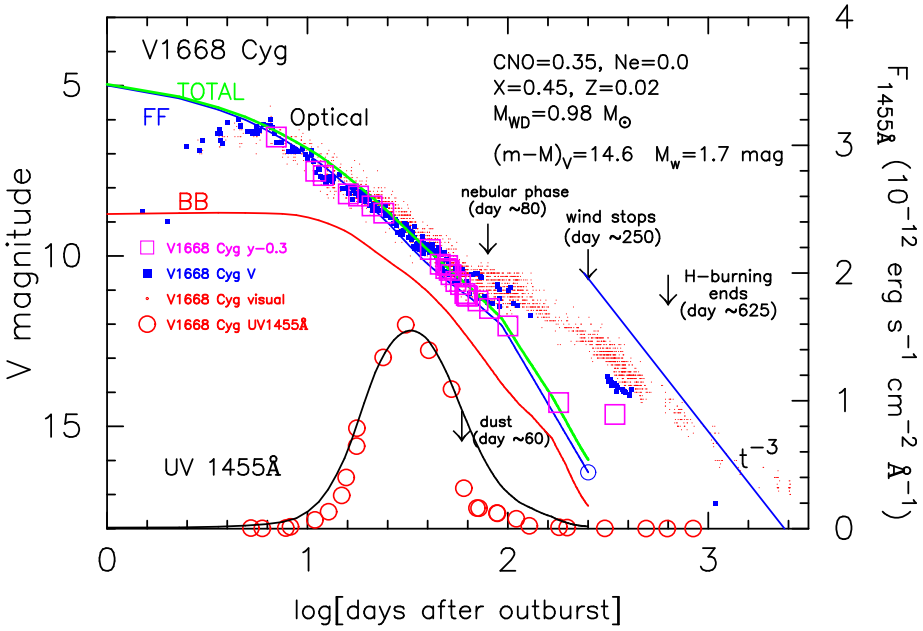

Figure 5: Model light curve fitting for V1668 Cyg with the chemical composition of CO nova 3. Assuming that $(m-M)_V = 14.6$, we plot three model light curves of the 0.98 $M_\odot$ WD. The green, blue, and red solid lines show the total (labeled "TOTAL"), free-free (labeled "FF"), and blackbody (labeled "BB") V fluxes. The black solid line denotes the UV 1455Å flux. An optically thin dust shell formed $\sim$ 60 days after the outburst [11]. Optically thick winds and hydrogen shell-burning end approximately 250 days and 625 days after the outburst, respectively, for the 0.98 $M_\odot$ WD model. The t^{-3} law (blue solid line) indicates the trend of free-free flux for a freely expanding nebula with no mass supply.

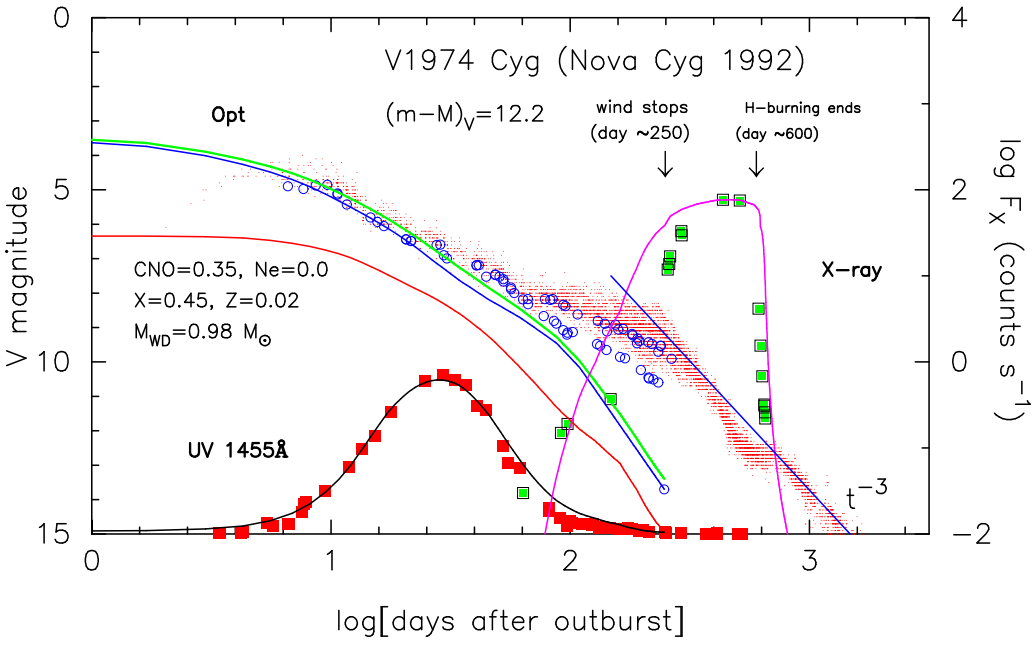

Figure 6: Same as Figure 4, but for V1974 Cyg.

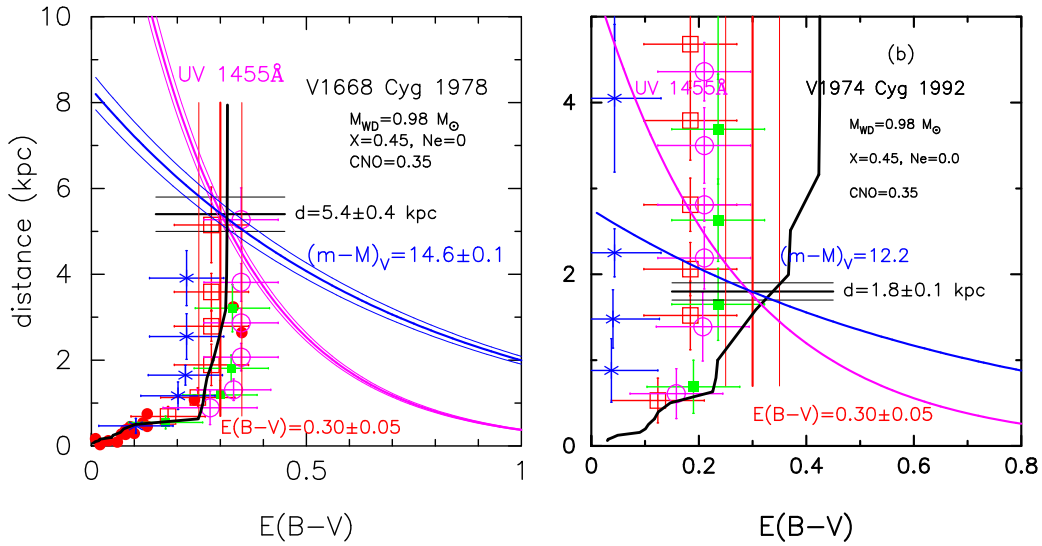

Figure 7: (a) Distance-reddening relations toward V1668 Cyg. The blue solid lines show the distance-reddening relations of $(m-M)_V = 14.6 \pm 0.1$. The magenta solid lines show the distance-reddening relations calculated from the UV 1455 Å flux fitting in Figure 5. We also plot other three distance-reddening relations toward V1668 Cyg. One is taken from Slovak et al. (1979) (red filled circles) and the others are relations given by Marshall et al. (2006): four directions close to V1668 Cyg, $(l,b) = (90.8373, -6.7598)$; that is, $(l,b) = (90.75, -6.75)$ (red open squares), $(91.00, -6.75)$ (green filled squares), $(90.75, -7.00)$ (blue asterisks), and $(91.00, -7.00)$ (magenta open circles), and given by Green et al. (2015) (black solid line). (b) Distance-reddening relations toward V1974 Cyg calculated from the V (blue solid lines) and UV 1455Å (magenta solid lines) light curve fittings in Figure 6. The red vertical solid lines show the reddening estimate of $E(B-V) = 0.3 \pm 0.05$, whereas the black horizontal solid lines correspond to the distance estimate of $d = 1.8 \pm 0.1$ kpc. We also show the distance-reddening relations given by Marshall et al. in four directions close to V1974 Cyg, $(l,b) = (89.1338, 7.8193)$, $(l,b) = (89.00, 7.75)$ (red open squares), $(89.25, 7.75)$ (green filled squares), $(89.00, 8.00)$ (blue asterisks), and $(89.25, 8.00)$ (magenta open circles). We also add Green et al.'s relation (black solid line).

we conclude that $d \sim 5.4 \pm 0.4$ kpc and $E(B-V) \sim 0.30 \pm 0.05$ for V1668 Cyg. This is consistent with the galactic dust absorption map of $E(B-V) = 0.29 \pm 0.02$ in the direction toward V1668 Cyg at the NASA/IPAC Infrared Science Archive[1].

We also obtain two distance-reddening relations to V1974 Cyg from the two model light curve fittings (V and UV 1455 Å) as shown in Figure 7(b). The thick blue solid line shows $(m-M)_V = 12.2 \pm 0.1$ and the thick magenta solid line shows the result obtained from the UV 1455Å flux fit in Figure 6. Figure 7(b) shows other distance-reddening relations toward V1974 Cyg: those are given by Marshall et al. [13] and Green et al.'s [14]. These trends are consistent with the cross at $d \approx 1.8$ kpc and $E(B-V) \approx 0.30$.

4. Application to slower novae

Figure 8 shows the light curve fit of our models with the observation of PW Vul. Our model light curves fit reasonably well with the observation for both the V and UV 1455Å bands. From the

[1] http://irsa.ipac.caltech.edu/applications/DUST/

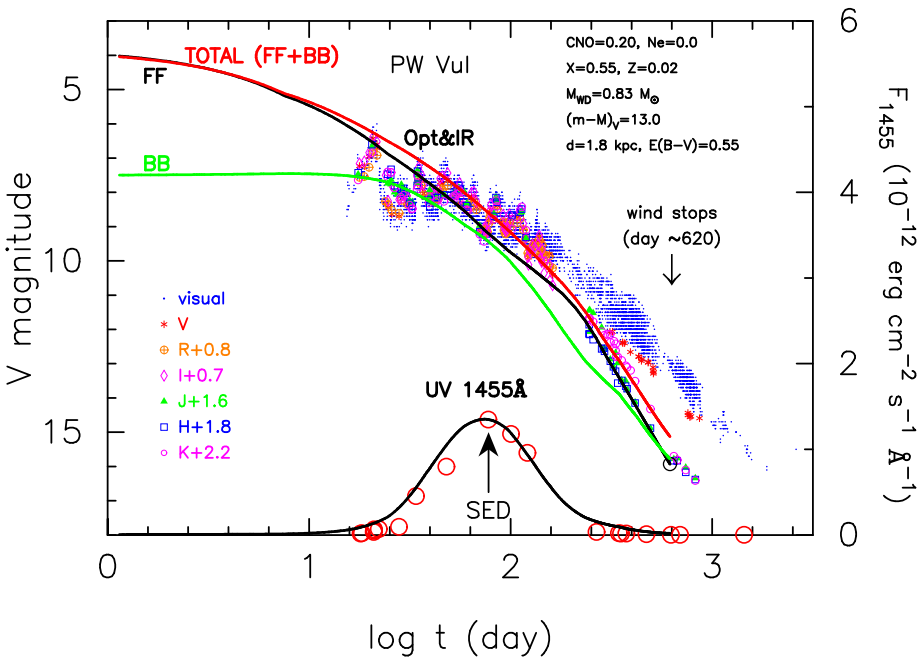

Figure 8: Model light curve fitting for PW Vul with the chemical composition of CO nova 4 (taken from Hachisu & Kato [9]). [9]). Red solid line denotes the total flux of free-free (black solid line) and blackbody (green solid line) emissions. Lower black solid line represents the UV 1455Å flux.

V and UV 1455Å light curve fittings of the 0.83 $M_\odot$ WD of the chemical composition of CO nova 4 ($X = 0.55$, $Y = 0.23$, $Z = 0.02$, and $X_{\rm CNO} = 0.20$) in Figure 8, we obtained $(m-M)_V = 13.0$ and $E(B-V) = 0.55$ (and the distance of $d = 1.8$ kpc). The photospheric emission is as large as that of free-free emission near 64 days after the outburst, in which the SED in Figure 1(b) was secured, and significantly contributes to the total flux. This is consistent with the decomposition of spectrum in Figure 1(b).

Figure 9 shows the light curve fit of our model light curves with the observation of V705 Cas. Our models fit reasonably well with the observation for both the V and UV 1455Å bands. From the V and UV 1455Å light curve fittings of the 0.78 $M_\odot$ WD of the chemical composition of CO nova 4 in Figure 9, we obtained $(m-M)_V = 13.4$ and $E(B-V) = 0.45$ (and the distance of $d = 2.5$ kpc). The photospheric emission significantly contributes to the total flux like in PW Vul.

Figure 10 shows the light curve fit of our models with the observation of V723 Cas. We assumed that the optically thick winds began to blow 155 days after the outburst [9]. Our model light curves fit reasonably well with the observation for both the V and UV 1455Å bands. From the V and UV 1455Å light curve fittings of the 0.51 $M_\odot$ WD of the chemical composition of CO nova 4 in Figure 10, we obtained $(m-M)_V = 14.0$ and $E(B-V) = 0.35$ (and the distance of $d = 3.9$ kpc). The photospheric emission dominates the optical bands. Thus, we may conclude that we must take into account the photospheric emission as well as the free-free emission to reproduce light curves of slow novae.

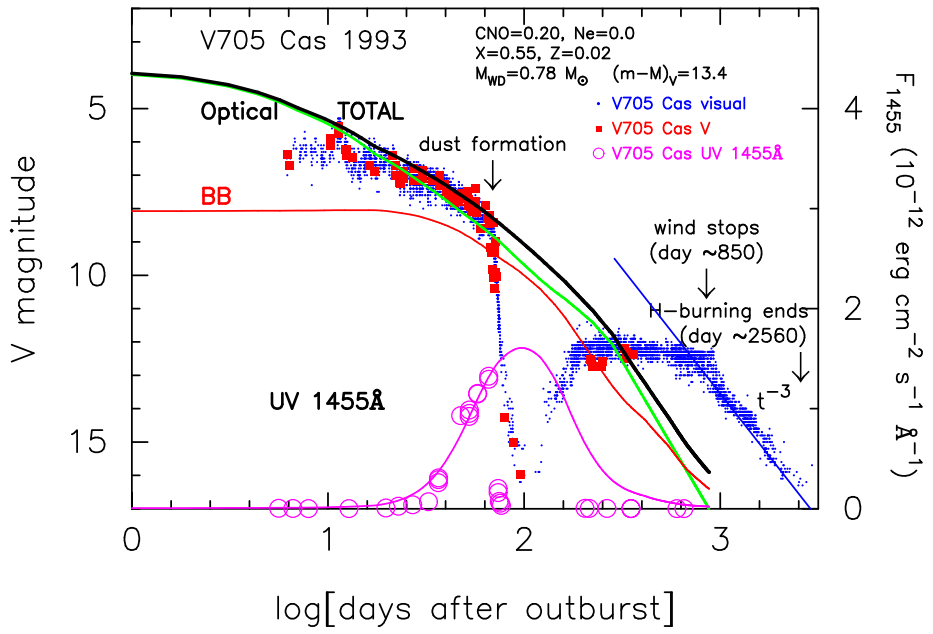

Figure 9: Model light curve fitting for V705 Cas with the chemical composition of CO nova 4 (taken from Hachisu & Kato [9]). Black line denotes the total flux of free-free (green solid line) and blackbody (red solid line) emissions. Magenta solid line represents the UV 1455Å flux.

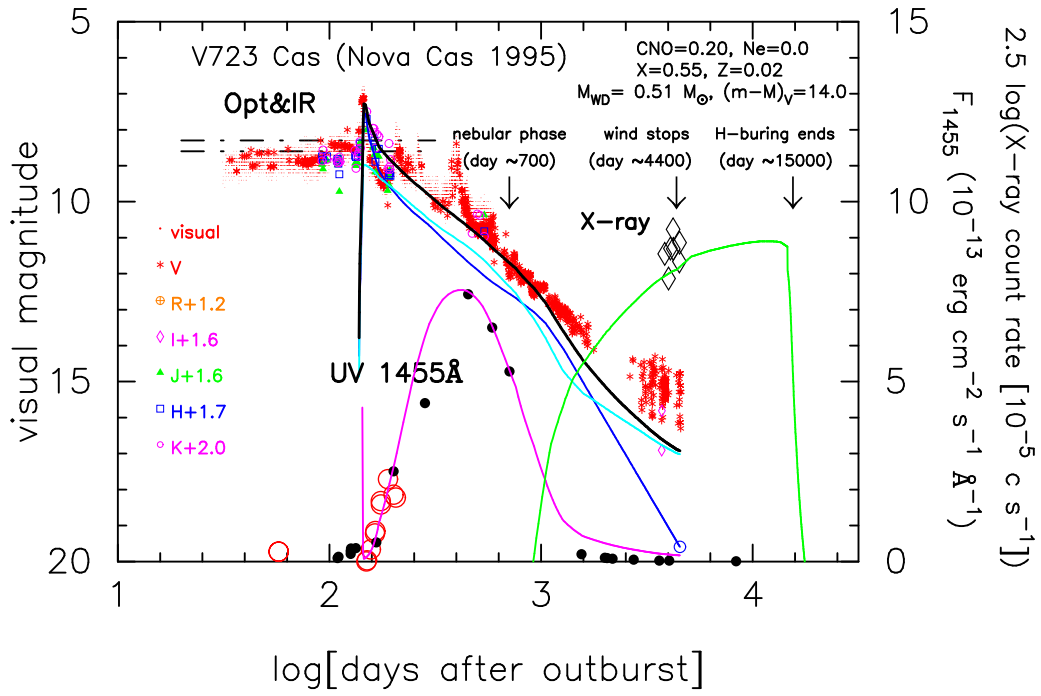

Figure 10: Model light curve fitting for V723 Cas with the chemical composition of CO nova 4 (taken from Hachisu & Kato [9]). Black line denotes the total flux of free-free (blue line) and blackbody (skyblue line) emissions. Magenta solid line represents the UV 1455Å flux.

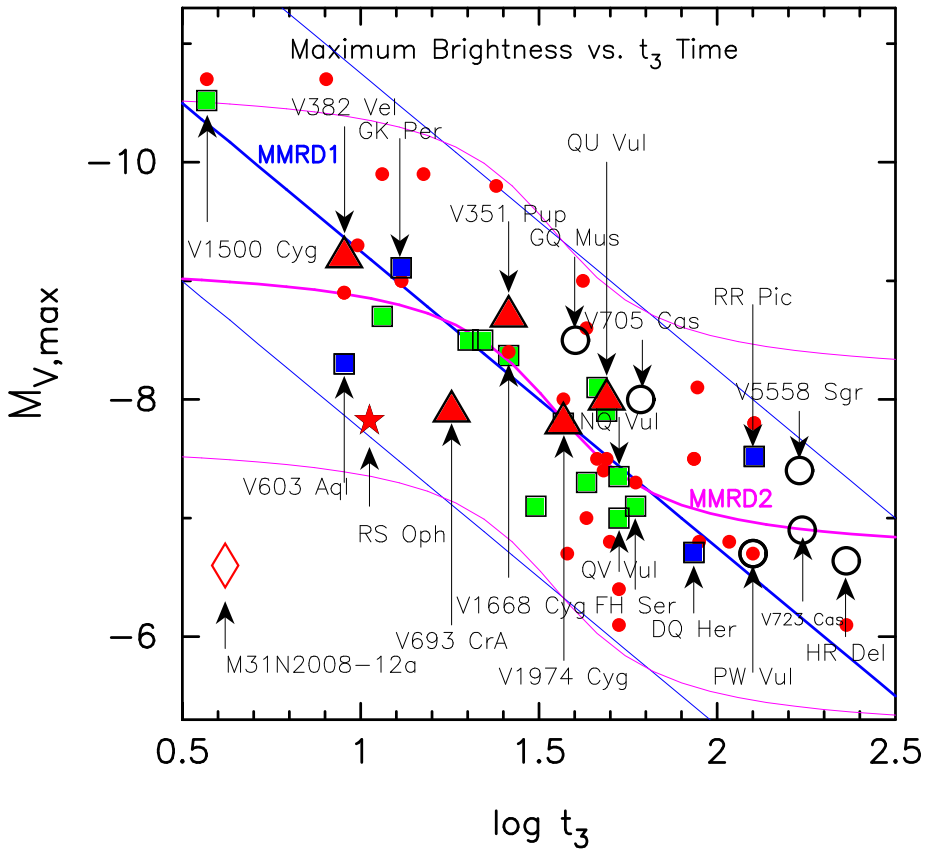

Figure 11: MMRD relations for various novae (taken from Hachisu & Kato [10]).

5. Maximum Magnitude vs Rate of Decline relation of novae

Using properties of the universal decline law, we can derive a theoretical MMRD relation. It should be emphasized that the MMRD relations are statistically derived from nova observation and the relation has a large scatter for individual novae. Hachisu & Kato [4, 9] claimed that the scatter of individual novae from the MMRD relation could be caused by (1) the difference in the ignition mass, i.e., the difference in the mass accretion rate, and by (2) the contribution of photospheric emission. In this section, we examine these effects for several examples.

Figure 11 shows observed data points of $(t_3, M_{V,\max})$ for many classical/recurrent novae. Red filled circles are novae taken from Downes & Duerbeck [17], the distances of which were mainly derived from the nebular expansion parallax method. We show six novae studied in Hachisu & Kato [5] by large black open circles, i.e., PW Vul, V705 Cas, GQ Mus, V5558 Sgr, HR Del, and V723 Cas. Green filled squares are novae taken from Hachisu & Kato [4], the distance moduli of which are determined by the time-stretching method. Blue filled squares indicate the four novae, V603 Aql, DQ Her, GK Per, and RR Pic, the distances of which were determined by Harrison et al. [18] with *HST* annual parallaxes. A blue solid line flanking with ± 1.5 mag lines indicates the relation of "Kaler-Schmidt's law" (labeled "MMRD1") [15]. A magenta solid line flanking with ± 1.5 mag lines indicates the relation of "della Valle-Livio's law" (labeled "MMRD2") [16].

Hachisu & Kato [1] found that nova light curves follow a universal decline law when free-

free emission dominates the continuum spectrum in optical and NIR regions. Using this property, Hachisu & Kato [4] found that, if two nova light curves overlap each other after one of the two is squeezed/stretched by a factor of f_s ($t' = t/f_s$) in the time direction, the brightnesses of the two novae obey the relation of $m'_V = m_V - 2.5\log f_s$. Based on this property, they derived a MMRD relation of $M_{V,\max} = 2.5\log t_3 - 11.6$ for the chemical composition of CO nova 2, in Hachisu & Kato [4]. We derived a similar trend, $M_{V,\max} = 2.5\log t_3 - 11.65$, for another chemical composition, CO nova 4, in Hachisu & Kato [9]. Note that these two relations are in good agreement with Kaler-Schmidt's law. The main trend of the MMRD relation is governed by the WD mass: the more massive a WD is, the steeper the decline of a nova light curve is. Hachisu & Kato [4] further showed that the maximum brightness of a nova also depends on the initial envelope mass (ignition mass). This initial envelope mass depends on the mass-accretion rate to the WD [19]. Hachisu & Kato [4] concluded that the scatter of individual MMRD points is due to various mass-accretion rates to the WD even for the same WD mass. The brighter the nova is, the smaller the mass accretion rate to the WD is [4].

Harrison et al. [18] pointed out that DQ Her and GK Per almost follow the MMRD relation (MMRD1) whereas V603 Aql and RR Pic do not. V603 Aql is located about 1 mag fainter than the blue solid line (MMRD1 relation). Hachisu & Kato [5] analyzed the light curves of V1500 Cyg and V603 Aql and concluded that both of these novae harbor a $\sim 1.2\ M_\odot$ WD for the same envelope chemical composition of Ne nova 2. We estimated the initial envelope masses for these two novae, that is, $M_{\rm env} = 0.92\times10^{-5}\ M_\odot$ for the $1.2\ M_\odot$ WD model of V1500 Cyg and $M_{\rm env} = 0.47\times10^{-5}\ M_\odot$ for V603 Aql. The initial envelope mass corresponds to the envelope mass at optical maximum. Thus, the difference in the ignition masses (i.e., mass accretion rates) makes the apparent difference in the start position (peak brightness) of outburst along the same model light curve (see Figure 40 of Hachisu & Kato [5]). This is the main source for scatter of individual MMRD points around the proposed MMRD relation. Therefore, a smaller initial envelope mass is the main reason that V603 Aql is fainter by ~ 1.2 mag than the blue solid line of MMRD1.

We further examine the case of PW Vul. The MMRD point of PW Vul is located slightly (0.2 mag) above Kaler-Schmidt's law (MMRD1), a blue thick solid line in Figure 11. Remember that our free-free emission model light curves usually follow the averaged MMRD relation of MMRD1 (Kaler & Schmidt's law). Thus, the agreement of PW Vul with the MMRD1 relation indicates that the initial envelope mass of PW Vul was a typical one for $\sim 0.83\ M_\odot$ WDs and also that free-free emission dominates the spectrum in V band.

The next is V705 Cas. This MMRD point is much (~ 0.8 mag) brighter than both of the MMRD1 and MMRD2 relations. As clearly shown in Figure 9, the photospheric emission is not as much to make the t_3 time longer by a factor of 2.0 (because $2.5\Delta\log t_3 = 2.5\log 2.0 \approx 2.5\times0.3 \approx 0.8$). Therefore, we attribute the difference in the maximum brightness to the difference in the initial envelope mass. To confirm this, we compared the rise time of UV 1455Å flux between PW Vul and V705 Cas in Figures 8 and 9. The UV 1455Å flux had already risen at the optical maximum in PW Vul while it had not yet in V705 Cas. The more massive initial envelope mass makes the brighter optical maximum of V705 Cas. Thus, it is located above the blue solid line of MMRD1 relation.

The position of V723 Cas is brighter than the blue solid line (MMRD1) by $2.5\Delta\log t_3 = 2.5\log 2.2 \approx 0.8$ mag. The photospheric emission contributes to make t_3 longer by a factor of

2.2. HR Del, V5558 Sgr, and RR Pic showed much brighter (~ 1.2 mag) optical maxima than the MMRD1 (blue solid line). These very slow novae showed prominent amplitudes of oscillations during the multiple-peak. We think that these large peaks are related to more massive envelopes compared with those of V723 Cas. In fact, the amplitude of multiple-peak is decreasing in V5558 Sgr, suggesting reduction of the envelope mass due to mass loss [9]. The same explanation is possible in RR Pic and HR Del, whose MMRD point is also 1.2 mag brighter than the MMRD1 relation (blue solid line).

It is interesting to see the position of the recurrent nova RS Oph (red filled star) and the 1 yr recurrence period M31 nova, M31N2008-12a (red open diamond) in Figure 11. RS Oph locates 1.2 mag below the MMRD1. This faintness corresponds to a much smaller envelope mass at optical maximum, suggesting a massive WD and very high mass accretion rate. This situation is very consistent with the total picture of recurrent novae; a very massive WD close to the Chandrasekhar mass and a high mass accretion rate to the WD [20]. The 1 yr recurrence period M31 nova, M31N2008-12a is depicted by a red open diamond. It is very faint, i.e., $M_{V,\max} = -6.6$ and $t_{3,V} \approx 3.8$ days [21]. The 1 yr recurrence period is close to the shortest recurrence period of novae, suggesting a very massive WD close to the Chandrasekhar mass and a very high accretion rate [19], thus a very small envelope mass. These support our conclusion that the peak brightness of a nova depends on the initial envelope mass as well as the WD mass itself.

To summarize, the primary parameter of the MMRD relation is the WD mass and the secondary parameter is the initial envelope mass. Variations in the initial envelope mass is the origin of scatter from the averaged MMRD relation, MMRD1. More massive envelopes correspond to the region above the MMRD1 line and less massive envelopes correspond to the region below the MMRD1 line. Photospheric emission is the third factor of the MMRD relation but becomes more important in slower novae, because it makes t_3 time longer in low mass WDs.

References

[1] Hachisu, I., & Kato, M. 2006, ApJS, 167, 59

[2] Cassatella, A., Altamore, A., & González-Riestra, R. 2002, A&Ap, 384, 1023

[3] Hachisu, I., & Kato, M. 2007, ApJ, 662, 552

[4] Hachisu, I., & Kato, M. 2010, ApJ, 709, 680

[5] Hachisu, I., & Kato, M. 2014, ApJ, 785, 97

[6] Hachisu, I., Kato, M., & Cassatella, A. 2008, ApJ, 687, 1236

[7] Kato, M., Hachisu, I., & Cassatella, A. 2009, ApJ, 704, 1676

[8] Kato, M., & Hachisu, I., 1994, ApJ, 437, 802

[9] Hachisu, I., & Kato, M. 2015, ApJ, 798, 76

[10] Hachisu, I., & Kato, M. 2016, ApJ, in press (arXiv:1511.06819)

[11] Gehrz, R. D., Hackwell, J. A., Grasdalen, G. I. et al. 1980, ApJ, 239, 570

[12] Slovak, M. H. & Vogt, S. S. 1979, Nature, 277, 114

[13] Marshall, D. J., Robin, A. C., Reylé, C., Schultheis, M., & Picaud, S. 2006, A&Ap, 453, 635

[14] Green, G. M., Schlafly, E. F., Finkbeiner, D. P., et al. 2015, ApJ, 810, 25

[15] Schmidt, Th. 1957, ZA, 41, 182

[16] della Valle, M., & Livio, M. 1995, ApJ, 452, 704

[17] Downes, R. A., & Duerbeck, H. W. 2000, AJ, 120, 2007

[18] Harrison, T. E., Bornak, J., McArthur, B. E., & Benedict, G. F. 2013, ApJ, 767, 7

[19] Kato, M., Saio, H., Hachisu, I., & Nomoto, K. 2014, ApJ, 793, 136

[20] Hachisu, I., & Kato, M. 2001, ApJ, 558, 323

[21] Darnley, M. J., Henze, M., Steele, I. A., et al. 2015, A&Ap, 580, A45

DISCUSSION

Joseph Patterson: T Pyx was missing in your gallery of slow novae. It appears to have an ordinary – not a high – mass for a nova. But it recurs very frequently. Why ?

Izumi Hachisu: The shortest recurrence period of T Pyx was 12 yr. Recent work of Kato et al. (2014, ApJ, 793, 136, Fig.6) shows that, if the WD mass of T Pyx is more massive than 1.15 $M_\odot$, it can recur every 12 yr for the mass accretion rate of 4×10^{-7} $M_\odot$ yr^{-1}. If we have the mass accretion rate of 1×10^{-7} $M_\odot$ yr^{-1} and recurrence period of 44 yr, the WD mass is about 1.1 $M_\odot$. These mass estimates from flash cycles are not consistent with $M_{\rm WD}=0.7\pm0.2$ $M_\odot$ claimed by Uthas et al. (2010, MNRAS, 409, 237).